CLM-R204

CLM-R204

UKAEA

Report

CULHAM LIBRARY
REFERENCE ONLY

X-RAY IMAGING OF JET A DESIGN STUDY FOR A STREAK CAMERA APPLICATION

J. E. BATEMAN
M. G. HOBBY

CULHAM LABORATORY
LIBRARY
- 2 FEB 1981

CULHAM LABORATORY
Abingdon Oxfordshire

1980

Available from H. M. Stationery Office

£2.00

© - UNITED KINGDOM ATOMIC ENERGY AUTHORITY - 1980
Enquiries about copyright and reproduction should be addressed to the Librarian, UKAEA, Culham Laboratory, Abingdon, Oxon. OX14 3DB, England.

CLM-R204

X-RAY IMAGING OF JET
A DESIGN STUDY FOR A STREAK CAMERA APPLICATION

J E Bateman*

and

M G Hobby
Culham Laboratory, Abingdon, Oxon, OX14 3DB, UK
(Euratom/UKAEA Fusion Association)

A single dimensional imaging system is proposed which will image a strip of the JET plasma up to 320 times per shot with a time resolution of better than 50 μs using the bremsstrahlung X-rays. The images are obtained by means of a pinhole camera followed by an X-ray image intensifier system the output of which is in turn digitised by a photodiode array. The information is stored digitally in a fast memory and is immediately available for display or analysis.

March 1980

*Physics Apparatus Group,
Instrumentation Division,
Rutherford and Appleton Laboratories
Chilton, Didcot
OXON

SBN: 0 85311 088 3

CONTENTS

1. Introduction

Given the rapid dependence of the intensity of the bremsstrahlung X-ray flux on critical plasma parameters (the density, temperature and impurity level) the benefit of imaging the plasma in the time domain by means of its soft X-ray radiation is very clear. Given also the high X-ray luminosity anticipated for JET, it would appear that sufficient signal may be available to image the fast fluctuations of the plasma distribution at frequencies around 10 kHz.

A cursory glance at the numbers involved shows that with fairly standard image intensifier techniques, a bidimensional X-ray image could be generated on a film or a TV system. However, the problem of extracting the vast quantity of information contained in a frame at rates of 10 kHz is virtually insoluble if it is to be done continuously for several milliseconds. If, on the other hand we restrict our requirement to a one dimensional or strip image of the plasma we find it immediately possible to frame at rates approaching 50 kHz with commercially available video digitising systems. In view of this fact and the belief that a vertical scan across the JET plasma will provide most of the desired information, the present design is restricted to producing a time sequence of one dimensional images (ie analogous to a streak camera). The technology which makes this possible consists of a photodiode array (PDA) of 100 elements (Integrated Photomatrix Ltd) reading out into a LeCroy video digitiser at 5 MHz, backed up by 32k words of store.

Two particular dimensions dominate the design of this instrument - (a) the plasma to pinhole distance - estimated to be $\sim$ 4 m and (b) the very small size of the PDA elements (0.1 mm x 0.1 mm). The former fact requires a large pinhole (for sensitivity) and therefore a large area X-ray detector to preserve spatial resolution, (say a field of $\sim$ 35 cm diameter with a 5 mm dia pinhole) and the latter fact requires a tiny image of 10 mm x 0.1 mm. The critical element of the design coupling these two dimensions is a demagnifying image intensifier (see figure 1). Various manufacturers make demagnifying X-ray image intensifiers

but the most suitable for our purposes would typically be one of the family made by Thomson CSF (THX413, THX497, THX1427).

While it is unlikely that the system described in this report can be fabricated from completely standard commercial items, it has been verified that the relatively minor modifications required to the image intensifiers and photo-diode array devices can be made by the manufacturers. Thus no major development programme on any item of the design is required. The areas where minor development is required will be indicated at the appropriate place in the text.

The main part of this report will consist of a linear presentation of the design shown schematically in figure 1. The detailed calculations will be found in the appropriate appendix.

2. The Streak Camera Design

Figure 1 shows the whole system in schematic form. The pinhole (chosen to be 5 mm in diameter) is assumed to be at a distance of 4 m from the centre of the plasma. Clearly a vacuum must be maintained in the X-ray flight path and a pumping rig must be supplied for this.

The pinhole camera optics are readily described (Appendix 2). The 5 mm pinhole transmits a factor of $\frac{1}{16}\left(\frac{5}{4000}\right)^2$ ($= 9.8 \times 10^{-8}$) of the X-rays emitted from a point source in the centre of the plasma. The magnification of the system may be chosen at will by moving the image plane. For reasons that will become evident we chose a magnification of 0.175 leading to an image distance of 700 mm and a spatial resolution (referred to the object plane) of $\left(1 + \frac{1}{0.175}\right)$ 5 mm = 33.5 mm.

The 100 cm diameter of the plasma thus reduces to 17.5 cm on the image intensifier front window.

Basing our design on the Thomson CSF tube type THX497 we find that it reduces the input field of 35 cm dia to 20 mm dia, ie a linear demagnification of 17.5:1. The image at the output window of the THX497 is now 10 mm in diameter and so matches the dimension of the PDA type IPL 7100. The second image

intensifier does not change the image dimensions but simply provides the necessary amplification for the PDA readout.

A point object in the plasma thus appears as a spot of 5(1 + 0.175) mm at the input of the THX497 and 5(1 + 0.175)/17.5 (= 0.335 mm) on the PDA (corresponding to 33.5 mm in the plasma).

Turning to the question of the sensitivity of the imaging system and the gain required from the image intensifiers (we note that the intensifiers simply constitute a transducer between an X-ray image and a visible light image) we find that the design process must begin with the PDA (see Appendix 4 for details). Each 0.1 mm x 0.1 mm element of the IPL 7100 array (there are 100 elements laid end to end) constitutes a capacitor which is charged on reset and discharged by incident light. The effective dynamic range is 5 pC with an overall noise of $\pm$ 2% and a sensitivity governed by a quantum efficiency (QE) of $\sim$ 25% in the middle of the visible spectrum. Most of the noise is fixed pattern (from the analogue gates in the readout shift register) and sensitivity fluctuations. If these are normalised out by suitable null-data runs stored in the computer, the residual 'white' noise in the readout is $\sim \pm$ 0.5% of full scale ie $\pm$ 0.025 pC. This, then, is the level to which we must compare the charge induced by a given exposure of a pixel to the plasma. Thus with an 8 bit ADC resolution, the readout noise is less than 1 significant bit.

The standard IPL 7100 has a plain glass window. One of the minor developments required is the replacement of this plain window by a fibre optic window (see Appendix 4). When this is done light can be coupled from the output face of the image intensifier into the PDA with an efficiency of about 10%. With a QE of 25% we can calculate the full scale deflection and noise figures in the PDA in terms of light flux at the output face of the image intensifier chain.

Thus 5 pC becomes $\dfrac{5 \times 10^{-12}}{0.1 \times 0.25 \times 1.6 \times 10^{-19}} = 1.25 \times 10^{9}$ photons

and the white noise is $\pm$ 6.7×10^{6} photons.

(These figures refer to a 0.1 mm x 0.1 mm pixel.)

Knowing the light signal required to drive the readout system we can now retrace our steps through the system and ascertain that the X-ray flux available from JET and the gain of the image intensifiers will produce this signal under the desired conditions.

Looking at figure 1 we see that the initial conversion of the X-rays into visible light takes place in a thin ($\sim$ 2 mg/cm^2) layer of CsI (Tl) scintillator evaporated on to the outside of the window of the THX497 image intensifier. Such layers are known to be as efficient as crystal scintillators, so given the QE of the tube ($\sim$ 18% at 420 mm) one can estimate that one will achieve $\sim$ 1.5 photoelectrons at the cathode per keV of incident X-ray energy. Poisson statistics then dictate that the detection efficiency of the system is $(1 - e^{-1.5E})$ where E is the X-ray energy.

A further term must be included for the absorption of the X-rays in the layer $(1 - e^{-\mu x})$. However this term is > 0.95 for energies below 6 keV for a 2 mg/cm^2 layer and so can be set to unity since there is little bremsstrahlung above 6 keV.

Before calculating the flux of photoelectrons generated at the cathode of the TXH497, one last factor must be taken into account, namely the active depth of the plasma. In the centre of the plasma image one looks at a projection some 100 cm deep. Thus for the brightest cm^2 of the image we assume that on average we are looking at some 50 cm^3 of plasma.

Thus the number of photoelectrons/s released by the image of 1 cm^2 of plasma in the image intensifier (II) is

$$\int_0^{2\ \text{keV}} 50 \times 5.3 \times 10^{13}\ E_p \frac{(1-e^{-\mu x})(1-e^{-1.5E})}{E} e^{-E/2} dE$$

As explained above $(1 - e^{-\mu x}) \sim 1$.

Ep = pinhole efficiency = 9.8×10^{-8}.

Thus we have $50 \times 5.3 \times 10^{13} \times 9.8 \times 10^{-8} \int_0^2 \frac{(1-e^{-1.5E})}{E} E^{-E/2} dE$

The integral is found to have the value 1.2.

ie $5 \times 5.3 \times 9.8 \times 1.2 \times 10^6$ X-ray signals (from 1 cm^2/s)

$= 3.12 \times 10^8 \ s^{-1}$.

Now because of the predominance of X-rays below 1 keV in the spectrum these signals consist essentially of 1 photoelectron and on the output face of the first image intensifier they all fall within a circle of 0.33 mm diameter. The light intensity generated by 1 cm^2 of plasma object at the output face plate is simply calculated as follows - each photoelectron receives 30 kV of energy and requires to spend $\sim$100 eV to generate a photon in the phosphor. Thus 3.12×10^8 events/s give $\frac{3.12 \times 10^8 \times 3 \times 10^4}{100}$ photons/s

ie 9.36×10^{10} photons/s into 4π.

Returning now to the sensitivity of the PDA as calculated above we note that FSD is 5 pC and requires $\sim 1.25 \times 10^9$ photons at the back of the first image intensifier ie peak white in the video image would require an exposure of $1.25 \times 10^9 / 9.36 \times 10^{10} = 0.013$ seconds and would contain $\sim 4 \times 10^6$ X-ray events integrated on a pixel. Clearly, in view of our requirement to image plasma fluctuations of 10 kHz this sensitivity is inadequate. If one adopts a sampling period of (say) 40 μs (the PDA readout can accommodate a scan as short as 20 μs) then an additional gain in the image intensifier system of some 0.013/0.00004 or 325 is required and peak white corresponds to a signal of 1.23×10^4 X-rays per pixel with a noise level of $\pm$ 62 X-rays.

The second image intensifier has the relatively easy task of supplying this low gain with no change in magnification. A 3 stage triode tube, conventional in all respects except that the usual slow P-20 phosphor must be replaced by a phosphor $\sim$1μs decay time (P15 or P24) will suffice for this task. (This is the other minor development which is required). One important (and fortunately readily available) design feature required of this image intensifier is that the final stage must have a high conductivity photocathode such as an S-20 with extended I.R. This arises because the high degree of demagnification

in our image leads to very high current densities in the image of the centre plasma. The quoted limit for an S-20 is 100μA/cm^2 and this corresponds to charging an element of the PDA to 1pC in 40μs.

We note in passing that the observed intensities per pixel will in practice be slightly greater than calculated above. This follows from the fact that while the image of a 1cm^2 source in the plasma overlaps a strip of ∿ 3 pixels with some loss at the edges, one pixel sees a circle in the plasma of ∿ 3.5 cm diameter (with varying solid angle). However, the degree of cancellation is such as to make the error small.

The above calculations may be summarised as follows.

1. The large pinhole (made possible by the large aperture image intensifier) gives very adequate X-ray fluxes on the CsI(Tℓ) crystal - viz ∿ 3 x 10^8 X-ray quanta from each cm^2 of image in centre plasma. This means that in an integration period of (say) 40μs we get ∿ 1.2 x 10^4 quanta in each pixel of the video. Thus statistical noise will be insignificant until the plasma brightness drops by more than a factor of 100 on this figure.

2. The gain of the image intensifiers is more than adequate to produce peak white in the video readout with X-ray fluxes of this order. In fact due to current density limitations in the final output stage of intensification we are restricted to ∿ 20% of peak in 40μs. However since the 'white' noise of the video is ∿ 0.5% of peak white, this is still a very clean signal. The gain necessary to image plasmas 100 - 1000 times fainter exists in the system.

The data capture electronics appear to present few problems. The circuits controlling the video scanning of the PDA are available very cheaply from IPL and only some minor control circuits are required in addition to permit selection of the integration period desired.

For the digitising of the video signal from the PDA it is proposed to use the Lecroy Model 8258 Video digitiser running at 5MHz with 32K 9 bit words of data storage. This permits 320 frames of plasma images to be stored with

an intensity resolution of 1 in 256 (the 9th bit is for frame synchronising). This system comes in CAMAC modules and it is proposed to control it via some suitable microcomputer (say an LSI-23). The IPL electronics produce a 5V dynamic range on the video signal while the Lecroy 8258 has a 512mV FSD, thus giving considerable latitude for accommodating fluctuations in the dynamic range. The display of the data could be arranged via a Graphics Output Controller and a TV monitor. Numerical analysis could be carried on in the LSI-23 or other data transmitted to another computer.

3. Conclusions

The X-ray streak camera design presented above provides a flexible system for digital imaging of the bremsstrahlung emission of the JET plasma on time scales from 20μs to 5ms per frame. Ample quantum statistics and image intensifier gain is available to produce noise free (quantified) images even at the shortest framing times. Spatial resolution in the plasma is ∿3.5cm and the field of view is 100cm x 3.5cm. Digital store for 320 frames is provided and control and display is foreseen via a microcomputer system with a graphics output controller and TV monitor.

The detailed calculations behind the arguments presented above, the technical specifications of the various pieces of equipment are detailed in the appendices. In particular the calculations on the various forms of shielding are reserved to appendix 8. It is therefore shown that, while the proposed system will operate satisfactorily in the JET environment, very substantial shielding will be required with the D-T neutrons, and this requirement will hold good for any detector system considered. The neutron flux at the detector site ($\sim 4 \times 10^{11}/cm^2/s$) is such as to flood any X-ray detector placed there. The energy detection efficiency of the scintillator for fast neutrons is $\sim 6 \times 10^{-3}$ so some 4 or 5 decades of attenuation are required to achieve acceptable noise rates ($\sim 10^4/cm^2/s$ of neutron induced noise). This represents some 1.5m of water shielding. Clearly the cost of the shielding

required will not be negligible.

It should be noted that the form of the intensifier chain suggested here is a recommendation of type and specification only. Other individual components may be equally acceptable.

Appendix 1 - Plasma Luminosity

The hydrogenic bremsstrahlung for a maxwellian plasma is given by the formula:

$$\frac{dN}{dE} = \frac{3\times10^{-15} N_e^{\,2}}{E\sqrt{T_e}} \exp\left(\frac{-E}{T_e}\right) \xi \text{ cm}^{-3}\text{s}^{-1}$$

where E is the X-ray quantum energy.

T_e is the electron temperature in keV

N_e is the plasma density

ξ is the enhancement factor due to impurities.

For the case of JET we take T_e = 2keV, $N_e = 5\times10^{13}$ cm^{-3}, ξ = 10.

$$\frac{dN}{dE} = \frac{3\times10^{-15}\ 25\times10^{26}}{E\sqrt{2}} \cdot \exp\frac{-E}{2} \cdot 10$$

$$= 5.3 \times 10^{13} \text{ cm}^{-3}\text{ s}^{-1} \quad \frac{\exp -E/2}{E}$$

$$\Delta N_{0.5-10\text{keV}} = 5.3\times10^{13} \int_{0.5}^{10} \frac{\exp -E/2}{E}\, dE$$

$$= 5.3\times10^{13} \text{ cm}^{-3}\text{ s}^{-1}$$

The image viewed by the pinhole camera is (of necessity) a projection of the plasma. Thus in the centre of the image we are looking at some 100 cm depth of plasma while at the edge only a few cm. For the brightness of the centre of the object, then, we can multiply by a factor which we choose as an average of ∿50 so that the numerical value of the object brightness in centre field is

$$\sim 2.65\times10^{15} \text{ cm}^{-2}\text{ s}^{-1}$$

Appended is a graph of the integral of the bremsstrahlung distribution formula with the lower limit of integration as the variable, (Fig.1.1).

$$y = f(A1) = \int_{A1}^{10} \frac{e^{-E/2}}{E} \, dE$$

where the electron temperature is assumed to be 2keV.

Appendix 2 - The Pinhole Camera

1. A pinhole camera has a transmission efficiency defined only by the solid angle subtended by the pinhole at the object

$$\text{thus Ec = camera efficiency} = \frac{1}{16}\ \frac{D^2}{U^2}$$

where D is the diameter of the pinhole and U is the object to pinhole distance.

Considering a 5mm dia pinhole at 4000 mm from the centre of the plasma we have

$$Ec = \frac{1}{16}\ \frac{25}{(4000)}^2$$
$$= 9.8 \times 10^{-8}$$

2. The magnification of a pinhole camera is determined solely by the ratio of the image distance to object distance.

ie

$$M = \frac{V}{U}$$

Making V=700 mm U=4000 mm M=0.175.

3. The spatial resolution of a pinhole camera referred to the object plane depends on the pinhole diameter and the magnification.

Thus

$$S = (1+\frac{1}{M})D$$

If M = 0.175 and D= 5 mm

$$S = 33.5 \text{ mm.}$$

Appendix 3 - Sensitivity of Image Intensifier System to X-Rays

1. Quantum Efficiency

The predominance of low energy X-ray quanta in the bremsstrahlung spectrum demands that a windowless detector should be used. Hence the decision to employ an evaporation of CsI(Tl) as a scintillator coupled to the first image intensifier. Bauer and Weingart have shown (IEEE Trans.Nuc. Sci. NS-15 (1968) No3 p 147) that the evaporations of both NaI(Tl) and CsI(Tl) give as much light output as crystalline scintillator. A thickness of 2 mg/cm^2 gives 90% detection efficiency at 6keV and below and CsI(Tl) is preferred because it is tolerant of exposure to the air. With a cathode QE in the II of ∿18% (60 mA/W @ 420 nm) and a CsI(Tl) scintillator we can anticipate ∿1.5 photo electrons per keV of X-ray energy deposited. Employing Poisson statistics we find that the detection efficiency of the scintillator -II combination (defined as the function of events incident which give rise to at least one photo electron) is

$$1 - Po \text{ where } Po = e^{-1.5E}$$

$$= 1 - e^{-1.5E} \quad (E \text{ being the X-ray quantum energy})$$

We should also multiply by the probability of absorption in the scintillator layer

$$= 1 - e^{-\mu(E)x}$$

However up to ∿6keV this is ∿1 and can be neglected for $\rho x \sim 2 mg/cm^2$
Now we note that the mean energy required to produce p.e. is 0.67 keV and the spectrum peaks vary strongly towards E=0, so most of the X-ray events will generate only one photoelectron.

We can now calculate the flux of photo electrons leaving the photo-cathode of the II due to 1 cm^2 of the plasma object.

$$\text{ie} \int_0^6 5.3 \times 10^{13} \times 50 \ \frac{\exp -E/2}{E} \times 9.8 \times 10^{-8} \ (1 - e^{-1.5E}) \ dE$$

The integral $\int_0^6 \frac{\exp -E/2}{E} (1 - e^{-1.5E}) \, dE$

has the value $\sim$ 1.2

ie we have 3.1×10^8 events/s containing $(3.1 \times 1.5 =) 4.65 \times 10^8$ photoelectrons per second leaving a circle $\sim$ 5 mm diameter on the photocathode due to a 1 cm^2 element of the plasma object.

Provided that enough gain can be obtained in the subsequent parts of the system, the quantum statistics exist in the primary signal at the first cathode to permit imaging in time slices down to a few microseconds.

2. Noise

The noise from the first photocathode is generally dominant in light amplifiers. The Thompson CSF tubes on which this design is based (THX 413, 497) have noise rates of $\sim$ 150 photoelectrons/s /cm^2, ie $\sim$ 100 X-ray events/s. This is about 10^7 down on the signal flux produced on the photocathode by a bright plasma.

3. Spatial Resolution

The spatial resolution obtained from the scintillator -II combination will be of the same order as the window thickness ($\sim$ 2 mm). This is smaller than the resolution of the pinhole camera ($\sim$ 5 mm). This is, of course, referred to the input face of the II. At the output face we have an image of the plasma demagnified by a factor of 17.5 (ideally) so that we are directly matched to the 10 mm length of the photodiode array (PDA). (The spatial resolution required is about 20 times poorer than the tubes are designed to yield.)

4. Tube Specification

The tube required for the front end II is identical to that developed by Thompson CSF for gamma camera applications. It is the front end of the THX 1427 system. An outline specification follows:-

Front window: 35 cm dia.

Back window (F10): 18-20 mm dia.

Demagnification (Electronic): 15-20.

EHT: 30 kV.

Input cathode sensitivity: $\gtrsim$ 60 mA/W @ 420 nm.

Spatial resolution referred to input: 0.5 lp/mm.

Input window thickness: $\lesssim$ 2 mm.

Output phosphor decay time: $\lesssim$ 5 μs.

5. The Second Image Intensifier

With the image of the plasma now $\sim$ 10 mm diameter it is easy to arrange the necessary amplification of the signal required to generate a few pC on each element of the PDA in some tens of microseconds. (The calculations are presented in the main text.) The type of tube envisaged to perform this role is a conventional 3 stage diode or triode tube with an overall photon gain of at least 10^3, 18-20 mm fibre optic windows, S-20 photocathodes, spatial resolution of $\gtrsim$ 3 lp/mm and a short decay phosphor ($\lesssim$ 5 μs). Such tubes are readily available from several manufacturers (eg Thompson CSF 9303) except that the normal phosphor is P-20 which is too slow for this system. This is one of the areas where some special development is called for.

6. High Flux Limitation

Problems arise when attempting to image in very short time slots due to the high intensity demanded of the final stage of the image intensifier chain. Let us assume that we require 1 pC of charge generated in 40 μs on one PDA pixel (10^{-4} cm^2). The number of electrons per cm^2 per sec flowing out of the pixel is thus

$$\frac{10^{-12}}{1.6 \times 10^{-19} \times 10^{-4} \times 4 \times 10^{-5}} = 1.56\ 10^{15}$$

Now the QE of the silicon is $\sim$ 0.2 and with fibre optic connections we can expect $\sim$ 10% collection efficiency. Thus the flux of photons at the output face of the final stage of image intensification is

$$\frac{1.56 \times 10^{15}}{0.02} = 7.8 \times 10^{16} \text{ photons/cm}^2\text{/s}.$$

With a 15 kV stage we may assume an electron to photon conversion gain of $\sim$ 150. Thus at the photocathode we have $\frac{7.8 \times 10^{16}}{150} \times 1.6 \times 10^{-19}$ amp/cm^2

$$= 83.2 \ \mu A/cm^2$$

This is within the 100 $\mu A/cm^2$ limit generally quoted for S-20 photocathodes.

It is thus one of the design constraints that a high current S-20 type photocathode is used in the final stage of intensification. This fortunately is the case in most commercial devices.

Appendix 4 - The Photodiode Array

It is proposed to use an array manufactured by IPL, the IPL 7100, which is a 100 element (each 0.1 mm x 0.1 mm) self-scanned linear array. IPL supply the electronic modules required to give charge readout on a 0 - +5V range corresponding to 0 - 5pC discharge of the elements. (PCM-74 and PCM-75.)

The responsivity of $10pC.S^{-1}.\mu W^{-1}.cm^2$ corresponds to a QE of $\sim$ 24% at λ = 600 nm (118 mA/W). No wavelength response curve is given but in general the QE of silicon deteriorates badly below 500 nm, so a blue phosphor on the output stage of the II should be avoided.

The noise is quoted as $\pm$ 2% of FSD (5pC). This is unacceptably large but is fairly easily improved since it comes from two main sources - (i) gate feed-through - which can be removed by subtracting the pedestals obtained with zero incident signal, and (ii) variation in sensitivity between diodes - which can be normalised by reference to a uniform exposure. With a correction table stored in the computer, the residual white noise is $\sim \pm$ 0.5% of FSD or better.

The IPL arrays are not normally provided with a fibre optic faceplate which is essential in this case. The manufacturers have agreed to make a batch with F/0 faceplates and the manufacturing uncertainties should give us a spatial resolution well within the 0.3 mm required. An order for 5 arrays is suggested to permit some experimentation with the specification and so achieve optimum results.

The only additional electronics required for reading the array will be a CAMAC module containing the necessary clock frequency generators to permit scanning for any arbitrary period. The diodes will not permit indefinite integration periods due to their intrinsic leakage. 5 ms is quoted as the maximum period at room temperature. However our 320 available frames take us out to 1.6 s - ie most of the JET pulse length.

Appendix 5 - Digitising and Data Storage

The design of this part of the system is facilitated by the availability of video digitisers. In particular we consider the LeCroy CAMAC based system. This consists of the 8258 (20 MHz) digitiser and the 8800 32k by 9 bit memory module. The ninth bit is reserved for frame synch. signals.

The 8258 requires only 512 mV for FSD so that there is scope for scale expansion with the +5V output of the PCM75.

This system will digitise the PDA signals at 5 MHz and at the end of an exposure present the data on command to an external computer or to a TV display via the Model 8658.

Appendix 6 - The Computer

It is envisaged that the streak camera will be controlled by a computer; in particular by an LSI-23 housed in the CAMAC crate. The LSI-23 plus an appropriate amount of memory will permit programming of the sweep frequency of the camera and control the display and storage of data. If analysis is to be performed on the data before display (eg fourier analysis) then a graphics output controller is desirable to give a flexible data display capability on a colour TV monitor.

Appendix 7 - Radiation Problems

Calculations recently made available indicate that when JET is operating with a D-T filling the neutron flux at the location of this detection system will be $\sim 4 \times 10^{11}$ fast neutrons/cm^2/s most of which have approximately 14 MeV of kinetic energy. This is an extremely intense neutron flux and corresponds to the typical core flux of a fission reactor, the only difference being that the neutrons are very much more energetic. We face three problems in this situation - (i) background induced in the detector by neutrons and the accompanying gamma flux, (ii) activation of the materials of the detection system, and (iii) radiation damage to the materials of the detection system. Let us consider these problems in reverse order.

1. Radiation Damage

Most materials start to show signs of radiation damage in the range of 10^{13}-10^{14} 14 MeV neutrons/cm^2. Thus we have roughly a lifetime of 100 JET shots for our system. The scintillator is likely to suffer most and fortunately it can be washed off and replaced. The only other vulnerable element is the PDA which also can be replaced. Eventually the glass of the image intensifiers will darken, but again this can be reversed to a certain extent by exposure to daylight. It would appear therefore that destruction of the device by radiation is not likely to be a problem even if no shielding is used; however as we shall see below, shielding is essential for other reasons.

2. Activation

All parts of the system are liable to become activated, but clearly activation of the scintillator is the most sensitive problem since this can lead to long term noise. Only the thermal part of the neutron spectrum can contribute to activation through the capture cross-section. The proportion of the spectrum which is thermal is almost totally dependent on the environment of JET. The more shielding we have the more thermal neutrons we will have.

Let us consider a pulse of N_o thermal neutrons/cm^2 from JET hitting our scintillator which we will consider element by element.

The number of excited nuclei produced will be

$$N_o \frac{N_A \sigma \rho x}{A} \quad (\text{per cm}^2)$$

N_A = Avogadro's No. σ = cross-section (cm^2), ρ = density (gm/cm^3), x = thickness (cm), A = gm atomic weight.

The counting rate resulting from this population is now

$$N_o \frac{N_A \sigma \rho x}{A} \frac{\log_e 2}{T_{\frac{1}{2}}} \quad \text{counts/cm}^2/\text{s}$$

where $T_{\frac{1}{2}}$ is the half life of the state concerned.

Evaluating the various constants we have

$$\text{Activity} = N_o \; 6.6 \times 10^{-6} \frac{\sigma}{T_{\frac{1}{2}}} \; \text{c/cm}^2/\text{s}$$

σ in barns $T_{\frac{1}{2}}$ in seconds.

The $^{127}I(n,\gamma)I^{128}$ reaction is the worst one in our cathode so we insert

$\sigma = 5.66$ $T_{\frac{1}{2}} = 1500$ s

when $A = N_o \times 2.48 \times 10^{-8}$ c/cm^2/s.

Betas and gammas deposit $\sim$ 10 keV ie 10 X-ray signals in the scintillator (see below) so we can expect to detect this noise if we get $\sim 10^5$ counts/s/cm^2 (the X-ray image goes up to $\sim 4 \times 10^8$ counts/cm^2/s) ie we need $\sim 10^{13}$ slow neutrons per shot to generate unacceptable noise.

However, the slow decay isotopes generated would steadily build up. Thus at 10^{13} slow neutrons/shot Cs^{134} ($T_{\frac{1}{2}}$ = 2.2y) would build up to an activity of 28,000 c/cm^2/s in 100 shots.

Such a flux of slow neutrons is many orders of magnitude ($\sim 10^5 - 10^6$) above what one could anticipate in the worst case so there would appear to be little

cause for concern. (At worst one would expect 10^{-4} of the 4×10^{11} $n/cm^2/s$ to thermalise.)

3. Radiation Induced Noise in the X-Ray Image

Fast neutrons (14 MeV) can produce an enormous range of interactions in materials from elastic scattering through (n,γ), (n,γ→e^-), (n,p), (n,d), to (n,α). However the bulk of the total cross-section in this region is the elastic process which also causes most trouble in that the recoils are densely ionising and can leave all their energy in the scintillator. Thus it is a worst case to assume that all neutron interactions with the scintillator are via elastic scattering.

The kinematics of Newtonian scattering tell us that the maximum recoil energy of an ion of mass M is

$$T_R = \frac{4Tn}{M}$$

The mean recoil energy is thus $\frac{2Tn}{M}$

with Tn = 14 MeV, M = 130 the mean recoil energy is ∿ 215 keV. Essentially all of this energy will be deposited in the layer but the saturation of the scintillation process by the high ionisation density will yield an X-ray equivalent of only ∿ $\frac{1}{3}$ ie ∿ 70 keV or 70 X-rays. Now the elastic scattering cross-section for most high Z materials lies in the range of a few barns and Cs and I are average at ∿ 5 barns at 14 MeV.

The attenuation coefficient for the fast neutrons is

$$\mu/\rho = \frac{N_A}{W}\sigma$$ where N_A = Avogadro's no.

W = Atomic wt.

σ = cross-section.

Substituting σ = 5 barns we get

$$\mu/\rho = 2.5 \times 10^{-2}\ cm^2/gm.$$

With a detector 2 mg/cm^2 thick we stop a fraction of an incident neutron beam

$$= \{1 - e^{-\frac{\mu}{\rho}(\rho x)}\}$$

$$\simeq \frac{\mu}{\rho}(\rho x) = 2.5 \times 10^{-2} \times 2 \times 10^{-3}$$

$$= 5 \times 10^{-5}.$$

Thus while the scintillator is $\sim$ 100% efficient for our X-rays it is only 5×10^{-3}% efficient for the neutron flux. However, we integrate the light signal so we must take account of the large light pulses given by the neutrons viz 70 keV per event. Our factor of 5×10^{-5} relative efficiency now increases to 3.5×10^{-3} ($5 \times 10^{-5} \times 70$). Clearly then it is important to keep the neutron flux at the image intensifier under control. If we assume that we have $\sim 10^8$ X-rays/s/cm^2 on the scintillator ($\sim$ 10% of the max flux) then to keep the neutron induced noise to 1% of this figure we must keep the neutron flux below $10^6/3.5 \times 10^{-3}$ or $\sim 3 \times 10^8$/cm^2/s.

Thus, given the quoted figure of 4×10^{11}/cm^2/s at our location, a factor of 10^3 in shielding must be obtained. As the attached data sheet shows this requires 115 cm of water or 130 cm of polythene, (Fig.7.2).

But we must also consider the unavoidable neutron flux hitting the scintillator through the pinhole. It is immediately clear from the sensitivity of the detector to the fast neutrons that only the slice of the plasma which it is desired to image must be allowed to shine neutrons on the detector. Thus a 2 cm wide slice is $\sim 10^{-3}$ of the plasma length and one would expect the flux at the detector to be $\sim 10^{-3}$ on the 4×10^{11}/cm^2/s value (assuming it is shielded from all other directions). This brings us to the acceptable region of $\sim 10^8$/cm^2/s. However we can improve the situation even further by filling in the unused cone of space around the pinhole with neutron absorber and perhaps win another reduction of a factor of 10^{-2} in the neutron flux. The attached figure shows what is required and indicates the scale of

the shielding, (Fig.7.1).

It is important to prevent thermal neutrons reaching the detectors, both from the noise aspect (thermal cross-sections are very large: $\sim 10^4$ barns) and the activation aspect. Therefore it is well to introduce a thermal neutron absorber (typically boron) into the shielding and put a cadmium screen around the tubes. However, these processes generate gamma rays of 0.4 - 1.5 MeV and therefore require $\sim$ 10 cm of lead as an inner shield. In this energy region $\sim$ 1 cm of lead halves the gamma flux. It is well known that composite shielding is much more efficient than single component types so that space can be saved at increased cost.

It is appropriate at this point to consider the sensitivity of the scintillator to the gamma rays which will be present from runaway electrons in JET but more important from neutron capture reactions in the shielding and environs. At about 0.5 MeV the gamma ray cross-section in CsI is $\sim$ 20 barns and this leads to an efficiency of $\sim 2 \times 10^{-4}$. The energy deposit by the induced fast electrons will be $\sim$ 10 keV per event. Thus the energy efficiency relative to the X-rays is 2×10^{-3}. This again implies that to stay below a noise signal of 10^6 keV/sec we require the gamma flux kept below $\sim 10^9/cm^2/s$. 10-15 cm of lead should suffice for this purpose. (See attached figure, Fig.7.3).

Appendix 8 - Magnetic and RF Interference

The magnetic field arising from the operation of JET is estimated to be $\sim$ 200G at the region occupied by the detector. This is clearly too much for the image intensifiers. However, a multiple mumetal screen will safety reduce the field to an acceptable level ($\lesssim$ 1G).

One advantage of this system is that the main stages of amplification are done in the light amplification mode and the only part of the system sensitive to RFI from the operation of JET is the PDA readout. This is a very compact system with small circuit boards holding the drivers (PCM 74/75) and it should be a relatively straightforward matter to adequately screen this part of the system.

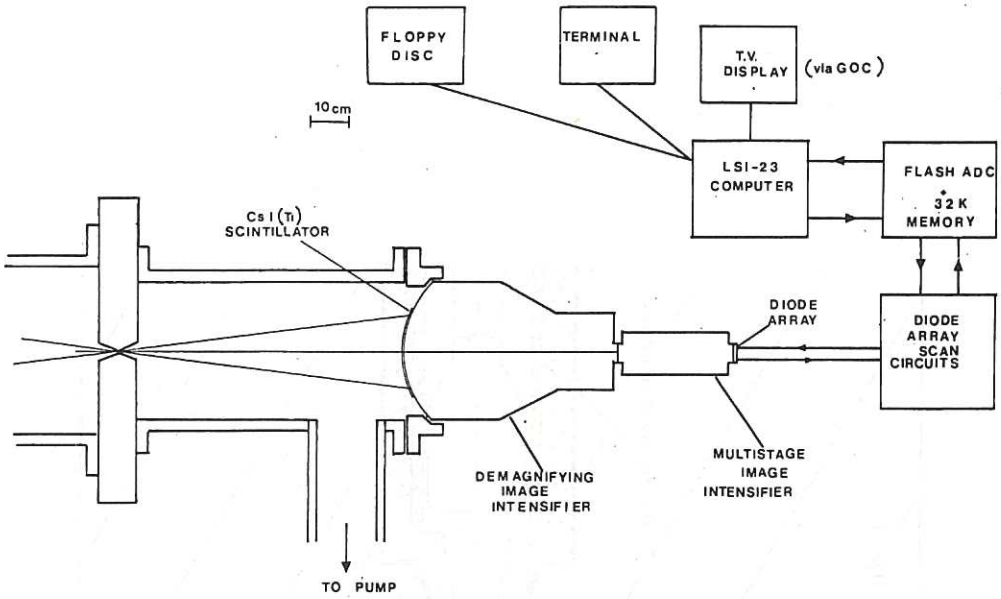

Fig.1 General schematic of the X-ray streak camera system showing the physical layout and electronic scheme.

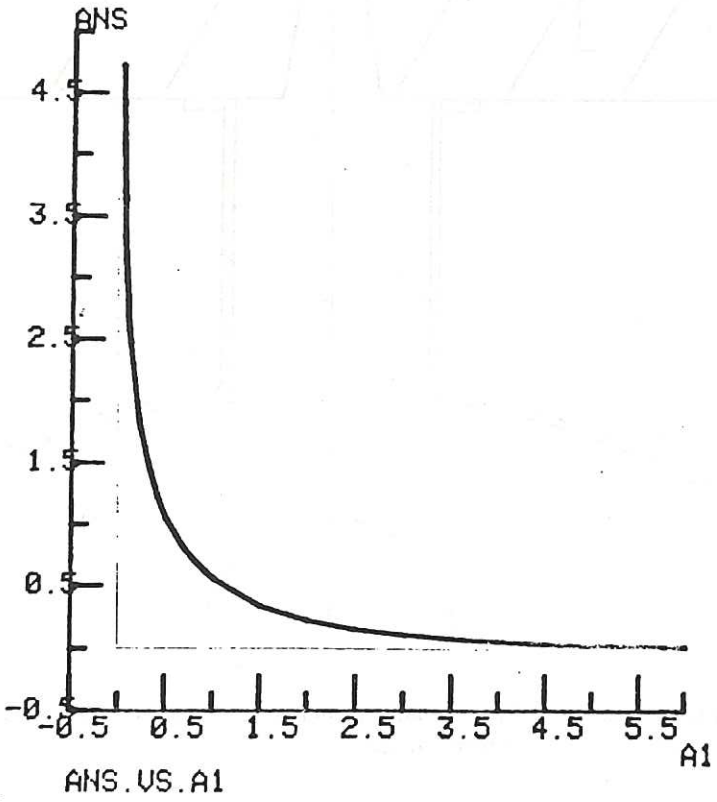

Fig.1.1 This figure shows a graph of the energy dependent part of the bremsstrahlung formula $(\frac{\exp -E/2}{E})$ as a function of the photon energy (E).

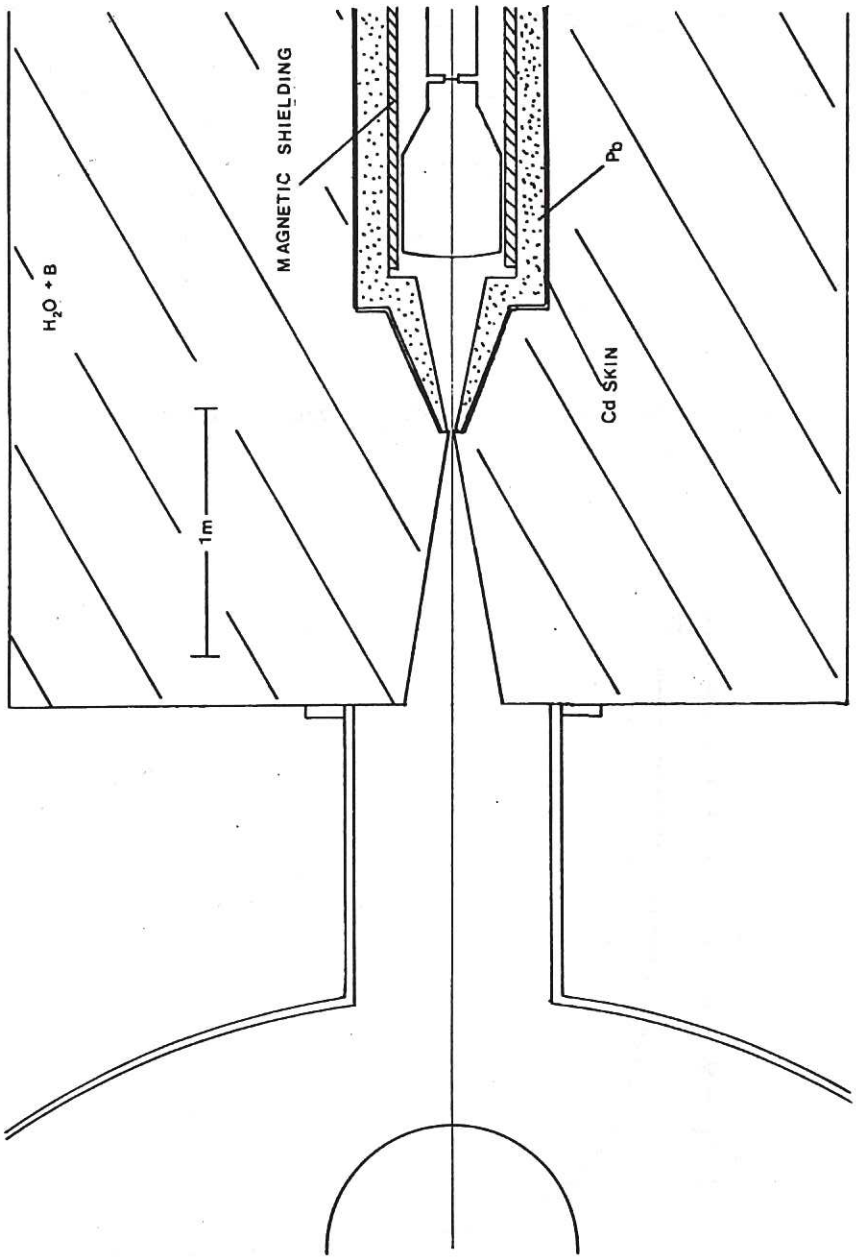

Fig.7.1 This figure shows a section of the shielding proposed to screen the streak camera from the ionising radiation background during the active phase of JET.

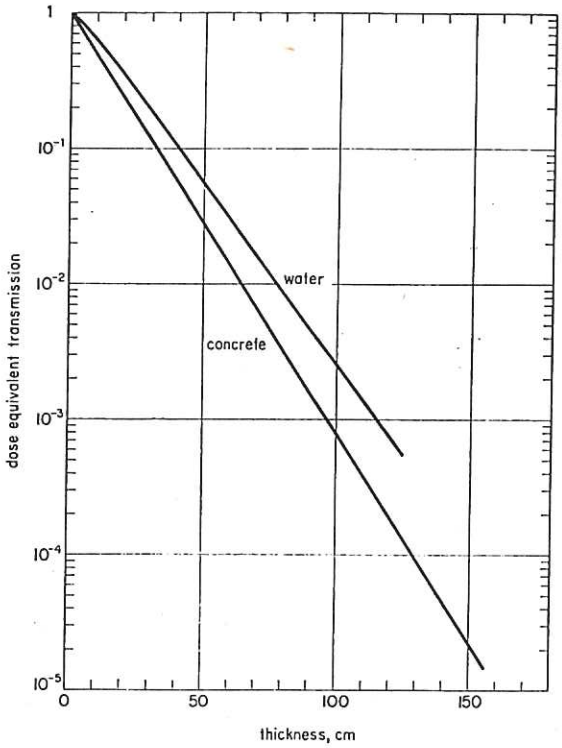

Fig.7.2 Broad-beam dose equivalent transmission of 14–15 MeV neutrons through slabs of concrete, density 2·4 g/cm^3, and water.

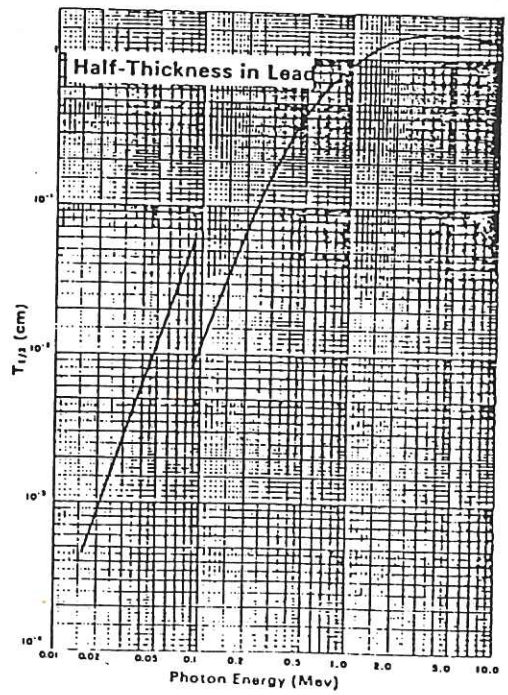

Fig.7.3 Half-thickness vs photon energy for lead. (Centimeters of lead of density 11·29 g/cm^3 necessary to reduce the number of gamma rays in a broad beam by a factor of 2.)

HER MAJESTY'S STATIONERY OFFICE

Government Bookshops

49 High Holborn, London WC1V 6HB
13a Castle Street, Edinburgh EH2 3AR
41 The Hayes, Cardiff CF1 1JW
Brazennose Street, Manchester M60 8AS
Wine Street, Bristol BS1 2BQ
258 Broad Street, Birmingham B1 2HE
80 Chichester Street, Belfast BT1 4JY

Government publications are also available through booksellers